

UNCLASSIFIED

AD _____

DEFENSE DOCUMENTATION CENTER

FOR

SCIENTIFIC AND TECHNICAL INFORMATION

CAMERON STATION ALEXANDRIA, VIRGINIA

DOWNGRADED AT 3 YEAR INTERVALS:
DECLASSIFIED AFTER 12 YEARS
DCD DIR 5200.10



UNCLASSIFIED

THIS REPORT HAS BEEN DECLASSIFIED
AND CLEARED FOR PUBLIC RELEASE.

DISTRIBUTION A
APPROVED FOR PUBLIC RELEASE;
DISTRIBUTION UNLIMITED.

AD No. ~~6673~~
ASTIA FILE COPY

APR 18 1953

Reproduced

FROM

LOW CONTRAST COPY:

ORIGINAL DOCUMENTS

MAY BE OBTAINED ON

LOAN

FROM

ARMED SERVICES TECHNICAL INFORMATION AGENCY

DOCUMENT SERVICE CENTER

U.B. BUILDING, DAYTON, 2, OHIO

**EFFECTS OF TEMPERATURE GRADIENTS,
SELF-ABSORPTION, AND SPECTRAL LINE-
SHAPE ON APPARENT ROTATIONAL
TEMPERATURES OF OH**

by

B. H. Elliott

**Daniel and Florence Guggenheim Jet Propulsion Center
California Institute of Technology
Pasadena, California**

**Technical Report No. 9
Contract Nonr-220(03), NR 015 210
Submitted by: S. S. Penner**

March 1953

**EFFECTS OF TEMPERATURE GRADIENTS,
SELF-ABSORPTION, AND SPECTRAL LINE-
SHAPE ON APPARENT ROTATIONAL
TEMPERATURES OF OH***

by

B. H. Elliott †

**Daniel and Florence Guggenheim Jet Propulsion Center,
California Institute of Technology
Pasadena, California**

The effects of temperature gradients, line contour, and self-absorption on observable intensities have been studied for the P_1 -branch, (0,0)-band, ${}^2\Sigma \rightarrow {}^2\Pi$ transitions of OH in absorption and emission experiments.

* Supported, in part, by the Office of Naval Research under Contract Nonr-220(03), NR 015 210.

† Lt. Colonel, U.S.M.C. This article is based, in part, on a thesis submitted by B. H. Elliott to the Graduate School of the California Institute of Technology, in partial fulfillment of requirements for the degree of Aeronautical Engineer. The author is indebted to Dr. S. S. Penner for helpful suggestions throughout the course of the work.

The effects on apparent rotational temperatures (of OH) of temperature gradients¹ and of spectral line-shape,² coupled with varying degrees of self-absorption,^{2,3} have been described for representative systems. It is the purpose of the present calculations to amplify the conclusions drawn previously in several respects by presenting additional numerical results particularly for simplified models of low-pressure and atmospheric - pressure flames.

The calculations emphasize the fact that definitive conclusions regarding interpretation of flame spectra are not easy to obtain by use of conventional low-resolution spectroscopic studies of flames. Multiple path experiments or absorption studies with discrete line sources appear promising provided they are restricted to conditions under which the spectral line-shape is known. Alternately, the use of interferometric studies may be indicated.

I. Effect of Line -Shape and of Self-Absorption on the Use of the Isointensity Method³ for Isothermal Systems.

According to the isointensity method the temperature of a radiator is obtained from a comparison of two spectral lines which are of equal intensity. Let $A(K)$ be the total intensity of the line identified by the

¹ S. S. Penner, "Quantitative Studies of Apparent Rotational Temperatures of OH in Emission and Absorption (Spectral Lines With Doppler Contour)", Technical Report No. 5, September 1952; Journal of Chemical Physics (in press).

² S. S. Penner, "Effect of Spectral Line-Shape on Apparent Rotational Temperatures of OH", Technical Report No. 8, November 1952; Journal of Chemical Physics (in press).

³ G. H. Dieke and H. M. Crosswhite, "The Ultraviolet Bands of OH, Fundamental Data," Bumblebee Series Report No. 87, Nov. 1948.

index K. Then, for spectral lines with Doppler contour,¹

$$A(K)/A(K') = \left[I_{\max}(K)/I_{\max}(K') \right] \left[\nu_{\ell u}(K)/\nu_{\ell u}(K') \right] \times \left[\xi(K')/\xi(K) \right] \quad (1)$$

where $I_{\max}(K)$ is the peak intensity emitted from the K'th line, $\nu_{\ell u}(K)$ is the frequency at the line center of the K'th line, and $\xi(K)$ is a known function of the value of $P_{\max} X$ for the K'th line, where P_{\max} is the maximum spectral absorption coefficient and X is the optical density. The line-shape for combined Doppler- and collision-broadening is described by the parameter

$$a = (b_N + b_C) (\ln 2)^{1/2} / b_D \quad (2)$$

where b_N , b_C , and b_D denote, respectively, the natural, the collision, and Doppler half-widths. In general $b_N \ll b_C$ and $a \approx 0$ for pure Doppler-broadening.

In order to emphasize that Eq. (1) applies to spectral lines with Doppler contour we shall write it as

$$A(a=0, K)/A(a=0, K') = \left[I_{\max}(a=0, K)/I_{\max}(a=0, K') \right] \times \left[\nu_{\ell u}(K)/\nu_{\ell u}(K') \right] \left[\xi(K')/\xi(K) \right] \quad (1a)$$

The effect of line-shape, under isothermal conditions, on the use of the iso-intensity method may be determined by evaluating the ratio $A(a, K)/A(a, K')$. This result can be obtained most conveniently by using Eq. (1a) in conjunction with the "curves of growth".⁴

⁴ E. M. F. van der Held, Z. Physik 70, 508 (1931); A. Unsöld, Physik der Sternatmosphären, p. 168, J. W. Edwards, Ann Arbor 1948; for an extension of the curves of growth to larger values of the line-shape parameter a , see S. S. Penner and R. W. Kavanagh, Technical Report No. 6, Contract Nonr-220(03), NR 015 210, California Institute of Technology, September 1952, or Journal of the Optical Society of America (in press).

The ordinate of the curve of growth is proportional to $A(a, K)$ for $P_{\max} X(K)$. Thus the ratio $A(a, K)/A(a = 0, K)$ can be obtained simply by reading the ordinate corresponding to the known value of $P_{\max} X(K)$. Finally, the quantity $A(a, K)/A(a, K')$ is obtained by writing

$$A(a, K)/A(a, K') = \left\{ \left[A(a, K)/A(a = 0, K) \right] / \left[A(a, K')/A(a = 0, K') \right] \right\} \times \left[A(a = 0, K)/A(a = 0, K') \right]. \quad (3)$$

The results for $K' = 1$ of representative calculations at $3000^\circ K$, using Eqs. (1a) and (3) together with the "curves of growth" [for the P_1 -branch of the $^2\Sigma \rightarrow 2\Pi$ transitions of OH, (0,0)-band], are plotted in Figs. 1 to 3 for $a = 0.005$, $a = 0.05$, and $a = 2$, respectively.* The self-absorption parameter \mathcal{E}' again refers to the value of $1 - \exp(-P_{\max} X)$ for the first line of the P_1 -branch and assumes the values 0.3, 0.7, and 0.95.

In order to illustrate the combined effects of line-shape and self-absorption on lines of equal intensity, from which conclusions might be drawn concerning the "temperature", the results listed in Table I may be consulted. In Table I the lines of intensity closest to the intensity for $K = 3$ and $K = 6$ have been tabulated for different values of \mathcal{E}' and of a . Reference to the data shown in Table I indicates a large effect of \mathcal{E}' for small a , but the results are quite insensitive to \mathcal{E}' for large a . Hence the conclusion is reached that self-absorption errors become more important as the pressure is reduced, i.e., as a is decreased. A more quantitative conclusion

* The authors ^{is} are indebted to Mr. N. Schroeder for performing the numerical calculations.

is justified only if absolute values are known for \underline{a} in flames, which is not the case at the present time.

Table I. Effect of $\underline{\epsilon}'$ and \underline{a} on Lines of Equal Total Intensity.

K value of line with intensity closest to $K = 3$ for			
	$\underline{\epsilon}' = 0.3$	$\underline{\epsilon}' = 0.7$	$\underline{\epsilon}' = 0.95$
$\underline{a} = 0.005$	13	14	16
$\underline{a} = 0.05$	13	14	16
$\underline{a} = 2$	13	13	14

K value of line with intensity closest to $K = 6$ for			
	$\underline{\epsilon}' = 0.3$	$\underline{\epsilon}' = 0.7$	$\underline{\epsilon}' = 0.95$
$\underline{a} = 0.005$	10	11	14
$\underline{a} = 0.05$	10	11	13
$\underline{a} = 2$	10	10	10

Because of the ambiguity in matching lines of equal intensity for small values of \underline{a} and large values of $\underline{\epsilon}'$ the isointensity method cannot be used, even for isothermal systems, at low pressures unless independent proof is provided that $\underline{\epsilon}' \ll 0.3$.

If $\underline{\epsilon}'$ is sufficiently small then it can be shown that

$$A(\underline{a}, K)/A(\underline{a}, K') = S_{\ell_u}(K)/S_{\ell_u}(K') \quad (4)$$

where $S_{\ell_u}(K)$ is the integral of the spectral absorption coefficient for the K 'th line. Here $S_{\ell_u}(K)$ is given by the expression⁵

⁵ S. S. Penner, J. Chem. Phys. 20, 507 (1952).

$$S_{\ell_u}(K) = (64\pi^4/3c^3) N_u(K) [\nu_{\ell_u}(K)]^4 [q_{\ell_u}(K)]^2 / c \rho^0[\nu_{\ell_u}(K)] \quad (5)$$

where c = velocity of light; N_u = number of molecules per unit volume per unit pressure in the upper energy state; ν_{ℓ_u} = frequency of the emitted or absorbed radiation at the center of the line, which is obtained from the Bohr frequency relation; q_{ℓ_u} = matrix element corresponding to transitions between the two given energy states; and $\rho^0(\nu_{\ell_u})$ = volume density of blackbody radiation at the frequency ν_{ℓ_u} as given by the Planck distribution law. The quantity $N_u(K)$ may be replaced by $N_u(K) = Ng_u(K) [\exp(-E_u(K)/kTu)] / Q$ where N = total number of molecules per unit volume per unit pressure, $g_u(K)$ = statistical weight of the upper energy state involved in the given transition, Q = complete partition function, and the expression for $S_{\ell_u}(K)$ may be rewritten as

$$S_{\ell_u}(K) = (64\pi^4/3c^3) Ng_u(K) [\nu_{\ell_u}(K)]^4 [q_{\ell_u}(K)]^2 \times \left\{ \exp[-E_u(K)/kTu] \right\} Q^{-1} c^{-1} \left\{ \rho^0[\nu_{\ell_u}(K)] \right\}^{-1} \quad (5a)$$

Hence, for lines of equal intensity,

$$\begin{aligned} S_{\ell_u}(K)/S_{\ell_u}(K') &= \left\{ [\nu_{\ell_u}(K)]^4 g_u(K) [q_{\ell_u}(K)]^2 \right\} \\ &\times \left\{ [\nu_{\ell_u}(K')]^4 g_u(K') [q_{\ell_u}(K')]^2 \right\}^{-1} \\ &\times \left\{ \rho^0[\nu_{\ell_u}(K')] \right\} \left\{ \rho^0[\nu_{\ell_u}(K)] \right\}^{-1} \\ &\times \exp \left\{ - [E_u(K) - E_u(K')] / kT_u \right\} \approx 1 \end{aligned} \quad (6)$$

But

$$\begin{aligned} \left\{ \rho^0[\nu_{\ell_u(K')}] \right\} \left\{ \rho^0[\nu_{\ell_u(K)}] \right\}^{-1} &= [\nu_{\ell_u(K')}]^3 [\nu_{\ell_u(K)}]^{-3} \\ &\times \left\{ \exp \left[h \nu_{\ell_u(K)} / k T_u \right] - 1 \right\} \\ &\times \left\{ \exp \left[h \nu_{\ell_u(K')} / k T_u \right] - 1 \right\}^{-1} \\ &\cong [\nu_{\ell_u(K')}]^3 [\nu_{\ell_u(K)}]^{-3} \\ &\times \exp \left\{ (h/k T_u) [\nu_{\ell_u(K)} - \nu_{\ell_u(K')}] \right\}. \end{aligned}$$

Substituting this relation in Eq. (6) we obtain

$$\begin{aligned} 1 &= [\nu_{\ell_u(K)} / \nu_{\ell_u(K')}] \left\{ g_u(K) [\nu_{\ell_u(K)}]^2 / g_u(K') [\nu_{\ell_u(K')}]^2 \right\} \\ &\times \exp \left\{ -[E_u(K) - E_u(K')] / k T_u \right\} \\ &\times \exp \left\{ (h/k T_u) [\nu_{\ell_u(K)} - \nu_{\ell_u(K')}] \right\} \end{aligned} \quad (6a)$$

In this last expression every quantity is known for a given pair of lines, except the temperature T_u . Hence Eq. (6a) can be used to obtain T_u as

$$T_u = - \frac{[E_u(K) - E_u(K')] + h[\nu_{\ell_u(K)} - \nu_{\ell_u(K')}]}{k \ln \left\{ \frac{[\nu_{\ell_u(K')}] g_u(K') [\nu_{\ell_u(K')}]^2}{[\nu_{\ell_u(K)}] g_u(K) [\nu_{\ell_u(K)}]^2} \right\}} \quad (6b)$$

This principle is used in conventional isointensity methods for measuring temperatures although the approximation $\nu_{\ell_u(K)} \approx \nu_{\ell_u(K')}$ is usually added.

It is clear from the preceeding discussion that the practical use of Eq. (6b) depends on the identity of $A(a, K)/A(a, K')$ with $S_{\ell_u(K)}/S_{\ell_u(K')}$. The limitations concerning this relation have been discussed in connection with Figs. 1 to 3 and Table 1.

II. Two-Path Experiments for Non-Isothermal Regions (Spectral Lines with Doppler Contour, Peak Intensities).

Calculations which are made in this section correspond to the assumed experimental arrangement illustrated in Fig. 4.

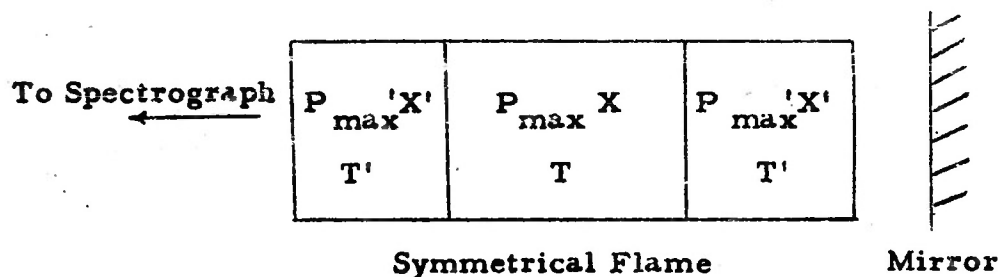


Fig. 4. Schematic arrangement of two-path experiment for a flame represented by two isothermal regions.

The OH concentration is treated as a variable parameter both in the hot region $\{\mathcal{E} = [1 - \exp(-P_{\max} X)]\}$ and in the cool region

$\{\mathcal{E}' = [1 - \exp(-P_{\max} X')]\}$. It is physically reasonable to assume $\mathcal{E}' \leq \mathcal{E}$.

Calculations have been carried out for peak intensities and for spectral lines with Doppler Contour. Peak intensities, even for low-pressure flames with Doppler-broadened lines, have not been measured. Such measurements might be possible with an interferometer. In particular, it is clear that the results of the present calculations do not apply to observational data obtained with a low-resolution spectrograph.

Referring to Fig. 4 the peak intensity I for the spectral line whose center lies at ν_{ℓ_u} may be written as follows:

$$\begin{aligned}
 I = & R'(\nu_{\ell u}) [1 - \exp(-P_{\max}' X')] + R(\nu_{\ell u}) [1 - \exp(-P_{\max} X)] \exp(-P_{\max}' X') \\
 & + R'(\nu_{\ell u}) [1 - \exp(-P_{\max}' X')] \exp(-P_{\max} X) \exp(-P_{\max}' X') \\
 & + r \left\{ R'(\nu_{\ell u}) [1 - \exp(-P_{\max}' X')] \exp(-2 P_{\max}' X') \exp(-P_{\max} X) \right. \\
 & + R(\nu_{\ell u}) [1 - \exp(-P_{\max} X)] \exp(-3 P_{\max}' X') \exp(-P_{\max} X) \\
 & \left. + R'(\nu_{\ell u}) [1 - \exp(-P_{\max}' X')] \exp(-2 P_{\max} X) \exp(-3 P_{\max}' X') \right\} \quad (7)
 \end{aligned}$$

where r is the reflectivity of the mirror and the other symbols have their usual meaning. Equation (7) may be rewritten in the form

$$\begin{aligned}
 I = & R'(\nu_{\ell u}) [1 - \exp(-P_{\max}' X')] \\
 & \left\{ 1 + \exp(-P_{\max} X - P_{\max}' X') + r \exp(-P_{\max} X - 2 P_{\max}' X') \right. \\
 & \left. + r \exp(-2 P_{\max} X - 3 P_{\max}' X') \right\} \\
 & + R(\nu_{\ell u}) [1 - \exp(-P_{\max} X)] \exp(-P_{\max}' X') \\
 & \left\{ 1 + r \exp(-P_{\max} X - 2 P_{\max}' X') \right\}. \quad (7a)
 \end{aligned}$$

Using Planck's blackbody distribution for $R(\nu_{\ell u})$ it follows that

$$R'(\nu_{\ell u})/R(\nu_{\ell u}) = \exp \left\{ - (h \nu_{\ell u}/k) \left[(1/T') - (1/T) \right] \right\}.$$

Hence Eq. (7a) becomes

$$\begin{aligned}
 I/R(\nu_{\ell u}) = & \left[1 - \exp(-P_{\max} X) \right] \exp(-P_{\max} X') \\
 & \left\{ 1 + r \exp(-P_{\max} X - 2 P_{\max} X') \right\} \\
 & + \exp \left\{ -(h\nu_{\ell u}/k) \left[(1/T') - (1/T) \right] \right\} \left[1 - \exp(-P_{\max} X') \right] \\
 & \times \left\{ 1 + \exp(-P_{\max} X - P_{\max} X') + r \exp(-P_{\max} X - 2 P_{\max} X') \right. \\
 & \left. + r \exp(-2 P_{\max} X - 3 P_{\max} X') \right\}. \quad (7b)
 \end{aligned}$$

For reasonable values of T and T' and for unit reflectivity of the mirror we obtain:

$$I \simeq R(\nu_{\ell u}) \mathcal{E} (1 - \mathcal{E}') \left[1 + (1 - \mathcal{E})(1 - \mathcal{E}')^2 \right] \quad (8)$$

If I' represents the intensity for the single path, then $I' \simeq R(\nu_{\ell u}) \mathcal{E} (1 - \mathcal{E}')$ whence

$$I/I' \simeq 1 + (1 - \mathcal{E})(1 - \mathcal{E}')^2. \quad (9)$$

The observable ratio I/I' has been calculated as a function of $\frac{K}{P_{\max} X}$ for various values of $\mathcal{E}(K=1)$ and $\mathcal{E}'(K=1)$ for the P_1 -branch and $^2\Sigma \rightarrow ^2\Pi$ transitions of OH. Results are plotted in Figs. 5 to 8.

Reference to Figs. 5 to 8 shows that the intensity ratio $I(K)/I'(K)$ is a very sensitive function of the self absorption parameters \mathcal{E} and \mathcal{E}' . It is clear that the intensity ratio for two-path experiments would be a much less sensitive function of \mathcal{E} and \mathcal{E}' for measurements of total intensity.

The important result derived from the present calculations is that even for values of \mathcal{E} as small as 0.3 the ratio $I(K)/I'(K)$ is appreciably less than two for the stronger lines. In other words, a

two-path experiment measuring peak intensities is a relatively sensitive device for studying self-absorption and temperature-distortion quantitatively. As will be shown in the following Section III, this last conclusion applies also to absorption experiments in which peak intensities are measured.

III. Absorption Experiment for Non-Isothermal Regions (Spectral Lines with Doppler Contour, Peak Intensities).

Because of the experimental difficulties arising from inadequate resolving power in the measurement of peak intensities for two-path experiments, it is of interest to consider the use of absorption experiments using discrete line sources.

Calculations which are made in this section correspond to the assumed experimental arrangement illustrated in Fig. 9. The light source radiates at the center of a given spectral line as a blackbody at the temperature T_s .

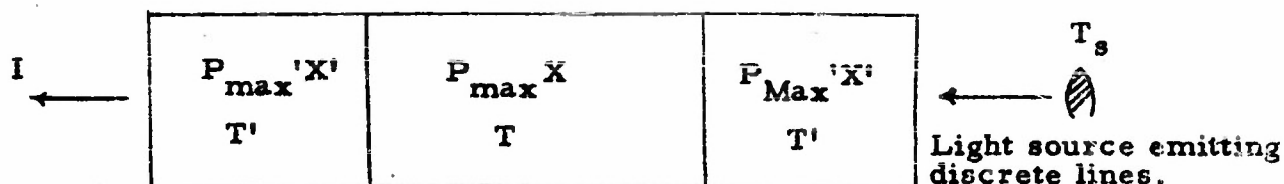


Fig. 9. Schematic arrangement of absorption experiment for a flame represented by two isothermal regions.

Referring to Fig. 9, the transmitted intensity I for the spectral line whose center lies at ν_{lu} may be written as follows:

$$\begin{aligned}
 I = & R(T_s) \exp(-2 P_{\max}' X' - P_{\max} X) \\
 & + R(T') \left[1 - \exp(-P_{\max}' X') \right] \\
 & + R(T) \left[1 - \exp(-P_{\max} X) \right] \exp(-P_{\max}' X') \\
 & + R(T') \left[1 - \exp(-P_{\max}' X') \right] \exp(-P_{\max} X - P_{\max}' X'). \quad (10)
 \end{aligned}$$

For $T_s \gg T, T'$ and $\exp(-P_{\max} X), \exp(-P_{\max}' X') \ll 1$,

$$I = R(T_s) \exp(-2 P_{\max}' X' - P_{\max} X). \quad (10a)$$

From Eq. (10):

$$\begin{aligned}
 I/R(T_s) = & \exp(-2 P_{\max}' X' - P_{\max} X) \\
 & + R(T')/R(T_s) \left[1 - \exp(-P_{\max}' X') \right] \left[1 + \exp(-P_{\max} X - P_{\max}' X') \right] \\
 & + R(T)/R(T_s) \left[1 - \exp(-P_{\max} X) \right] \exp(-P_{\max}' X') \quad (10b)
 \end{aligned}$$

or

$$\begin{aligned}
 I/R(T_s) = & \exp(-2 P_{\max}' X' - P_{\max} X) \\
 & + \exp \left\{ -(h \nu_{\ell u}/k) \left[(1/T') - (1/T_s) \right] \right\} \left[1 - \exp(-P_{\max}' X') \right] \\
 & \times \left[1 - \exp(-P_{\max} X - P_{\max}' X') \right] \\
 & + \exp \left\{ -(h \nu_{\ell u}/k) \left[(1/T') - (1/T_s) \right] \right\} \left[1 - \exp(-P_{\max} X) \right] \exp(-P_{\max}' X'). \quad (10c)
 \end{aligned}$$

In general we may neglect the radiation from the region at temperature T' and use the relation

$$\begin{aligned}
 I/R(T_g) &= \exp(-2 P_{\max}' X' - P_{\max} X) \\
 &+ \exp\left\{- (h \nu_{\ell u}/k) \left[(1/T) - (1/T_g) \right] \right\} \left[1 - \exp(-P_{\max} X) \right] \exp(-P_{\max}' X') \\
 &= (1 - \epsilon')^2 (1 - \epsilon) + \epsilon (1 - \epsilon') \exp\left\{- (h \nu_{\ell u}/k) \left[(1/T) - (1/T_g) \right] \right\}. \quad (10d)
 \end{aligned}$$

If $T_g \gg T$, as should be the case for a good absorption experiment, then

$$\exp\left\{- (h \nu_{\ell u}/k) \left[(1/T) - (1/T_g) \right] \right\} \simeq \exp(-h \nu_{\ell u}/kT).$$

But $h \nu/k = hc\omega/k = 1.432\omega$ and $\exp(-h \nu_{\ell u}/kT) \simeq \exp(-1.432 \times 30,000/3000) \simeq \exp(-14)$.

Hence for $T_g \gg T$ Eq. (10d) may be written as

$$I/R(T_g) \simeq (1 - \epsilon')^2 (1 - \epsilon). \quad (11)$$

Comparison of Eqs. (9) and (11) shows that the transmitted intensity divided by the incident intensity from a discrete line source is nearly equal to $I/I' - 1$ where I/I' is the ratio of the intensity of the flame for a double-path experiment to the intensity of the flame for a single-path experiment. Figures (5) to (8) may then be reinterpreted in such a way that $I/I' - 1$ represents the absorptivity of the flame for discrete radiation.

Since I/I' or $I/I' - 1$, for measurements of peak intensities, are very sensitive functions of the self absorption parameters ϵ and ϵ' , it follows that $I/R(T_g)$ is also a sensitive function of ϵ and ϵ' . Unlike peak intensity determinations in two-path experiments, the discrete line source experiment may be feasible with ordinary spectroscopic apparatus by using as source OH in a discharge tube or else an excited

metal line which coincides exactly with a line of OH. * In this connection it is of interest to note that the 3063.978 Å line of tungsten coincides with the 10' line of the (0, 0) band, $^2\Sigma \rightarrow ^2\Pi$ transitions of OH.

IV. Two-Path Experiments for Non-Isothermal Regions (Spectral Lines with Combined Doppler and Collision Broadening; Peak Intensities).

The calculations summarized in this section again correspond to the experimental arrangement illustrated in Fig. 4 of Section II. The parameter P_{\max} must now be replaced by $P(\omega_{\ell u})$ where $P(\omega_{\ell u})$, the spectral absorption coefficient at the line center, is to be evaluated for combined Doppler- and collision-broadening. The quantity $P(\omega_{\ell u})$ is related to P_{\max} and a through the expression⁴

$$P(\omega_{\ell u}) = P_{\max} \left[\exp(a^2) \right] \left[\operatorname{erfc}(a) \right] \quad (12)$$

where

$$\operatorname{erfc}(a) = \left[2/\pi^{1/2} \right] \int_a^{\infty} \left[\exp(-x^2) \right] dx.$$

Equation (9) may be rewritten as

$$I/I' \approx 1 + (1 - \mathcal{E}_{D-C})(1 - \mathcal{E}'_{D-C})^2 \quad (9a)$$

where

$$\mathcal{E}_{D-C} = 1 - \exp \left[-(P_{\max} X) \operatorname{erfc}(a) \exp(a^2) \right], \quad (13)$$

$$\mathcal{E}'_{D-C} = 1 - \exp \left[-(P_{\max}' X') \operatorname{erfc}(a') \exp(a'^2) \right], \quad (13a)$$

and a' represents the line-shape parameter for the gases at the temperature T' .

* Absorption experiments using discrete lines as source have been considered at various times by most of the active workers in combustion spectroscopy.

The ratio I/I' has been calculated for $a' = a$ ranging from 0 to 10, $\epsilon(K=1) = 0.7$, $\epsilon'(K=1) = 0.1$ and 0.5 , for the P_1 -branch, $(0,0)$ -band and $^2\Sigma \rightarrow ^2\Pi$ transitions of OH. Results are plotted in Figs. 10 and 11. Reference to Figs. 10 and 11 shows that two-path experiments will yield results which are sensitive functions of the line-shape parameter a , with distortion of experimental data by self-absorption diminishing as the numerical value of a is increased, under otherwise comparable experimental conditions.

V. Peak Absorption Experiments for Non-Isothermal Regions
(Spectral Lines with Combined Doppler and Collision Broadening)

Calculations in this section correspond to the experimental arrangement illustrated in Fig. 9 of Section III with P_{\max} replaced by $P(\omega_{lu})$. Here $P(\omega_{lu})$ again depends on P_{\max} and a as shown in Eq. (12).

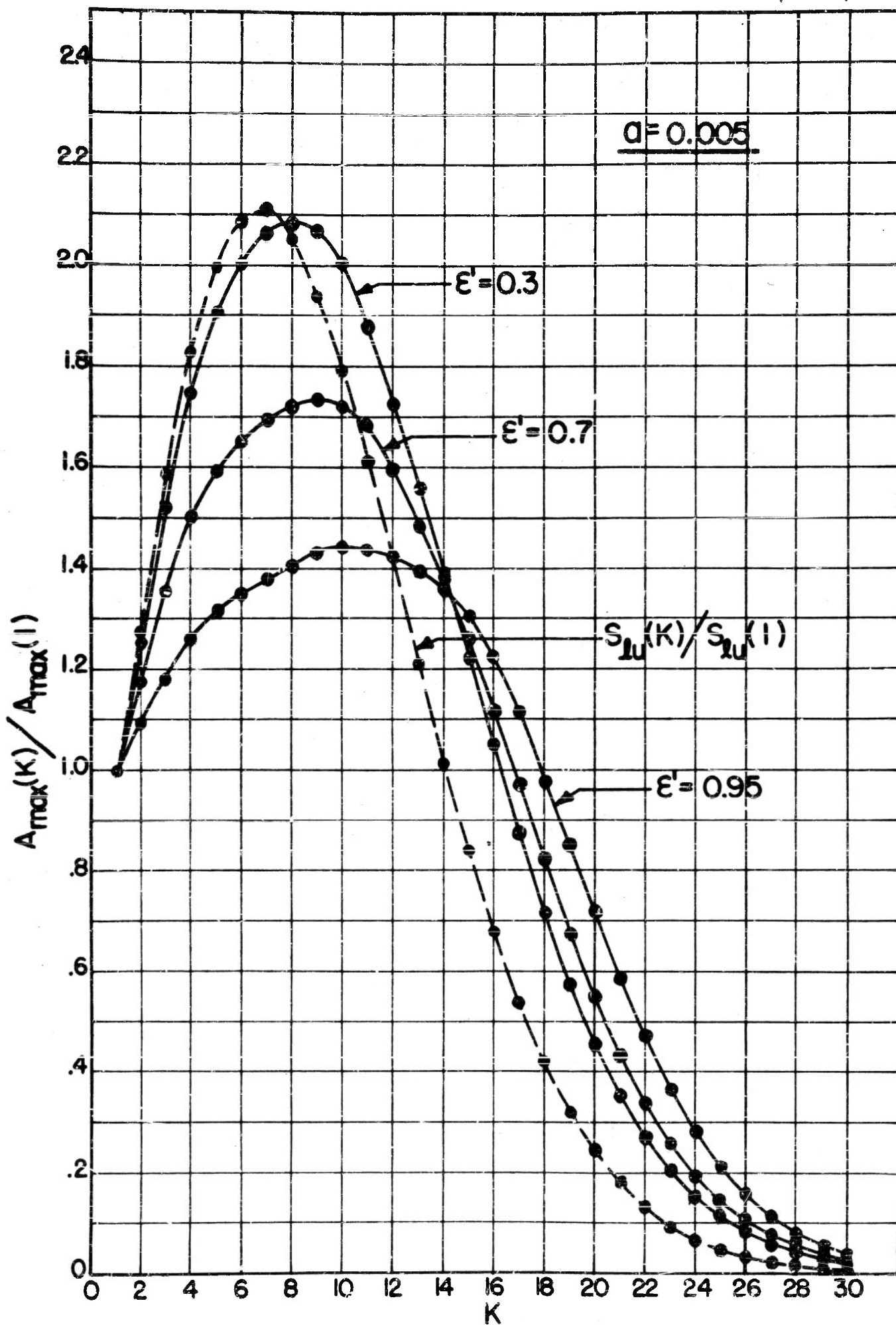
Equation (11) now becomes

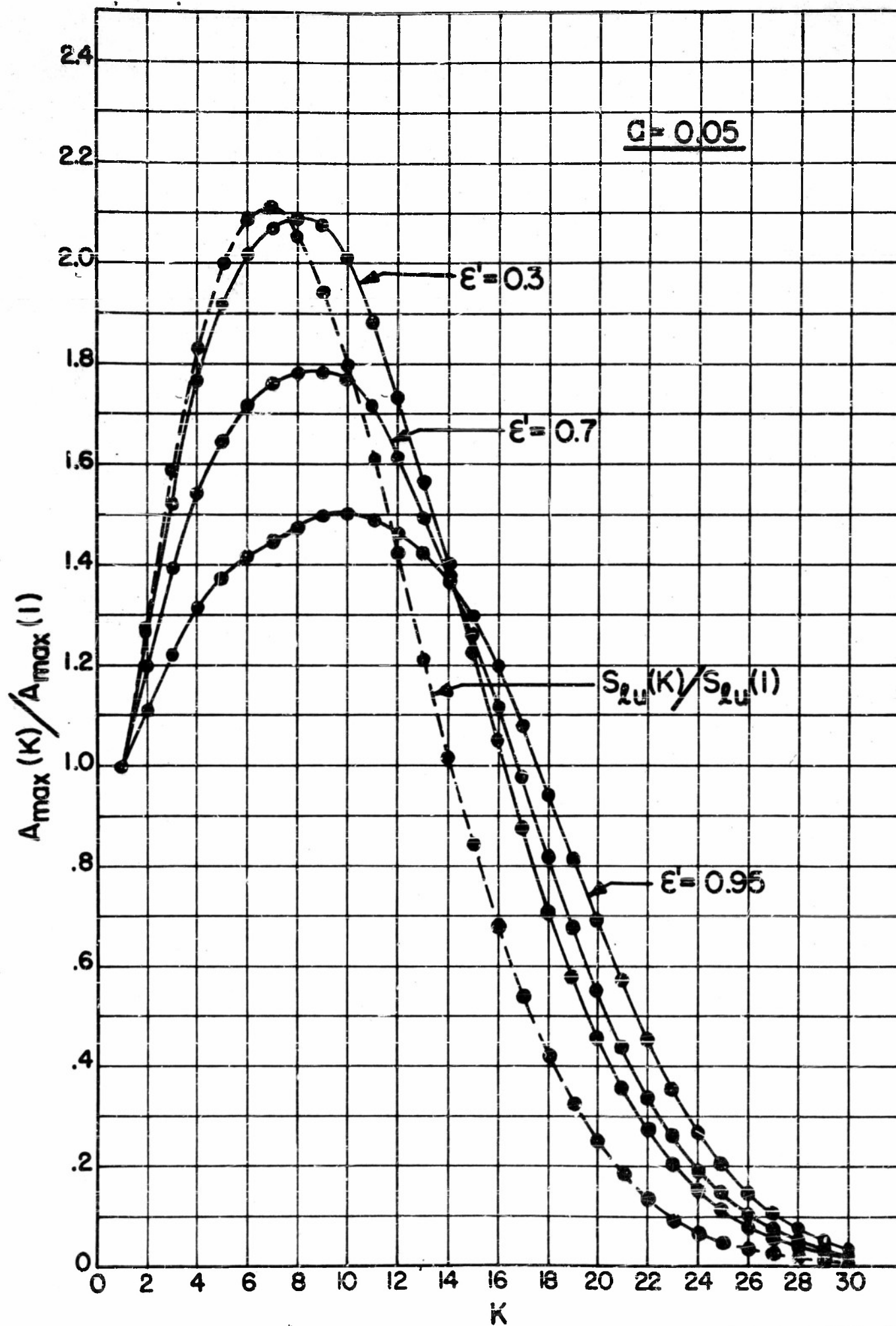
$$I/R(T_g) \simeq (1 - \epsilon_{D-C})(1 - \epsilon'_{D-C})^2 \quad (11a)$$

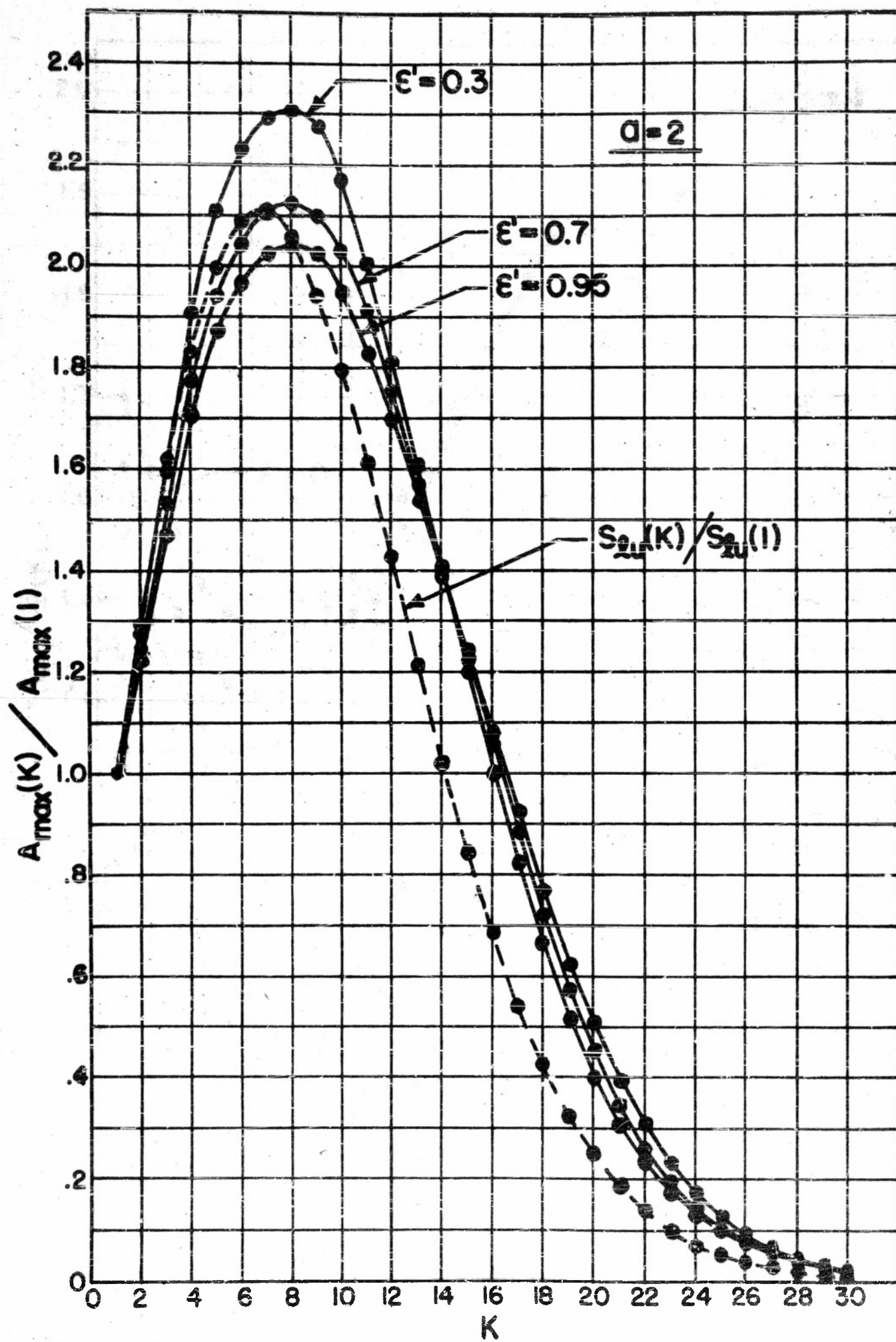
where ϵ_{D-C} and ϵ'_{D-C} have been defined in Eqs. (13) and (13a). Comparison of Eqs. (9a) and (11a) shows that $I/RT_g = I/I' - 1$ is obtained simply by reinterpreting the ordinates of Figs. 10 and 11. Hence the same conclusions apply to absorption experiments with discrete sources as to measurements of peak intensities for two-path experiments.

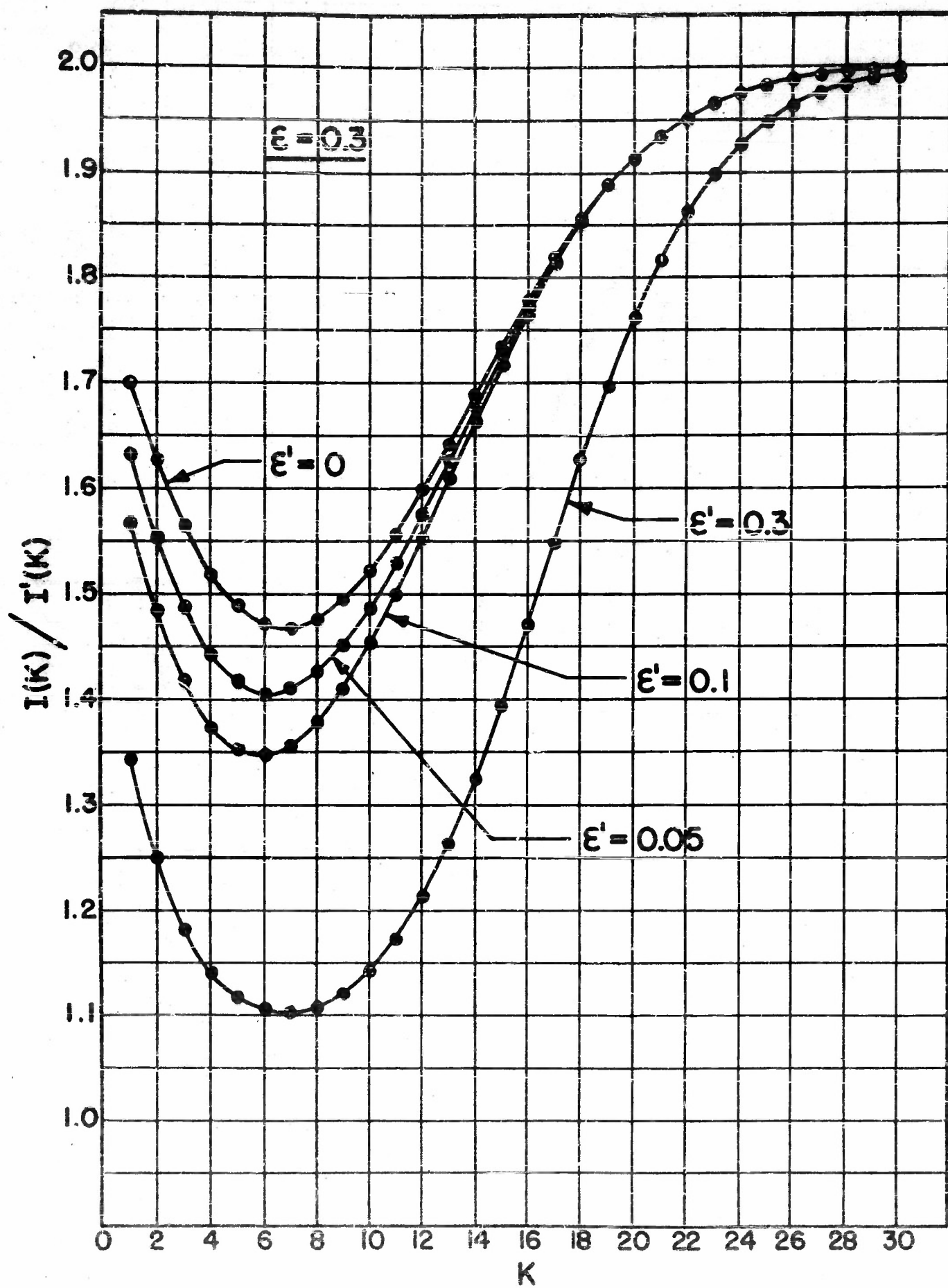
LIST OF FIGURES

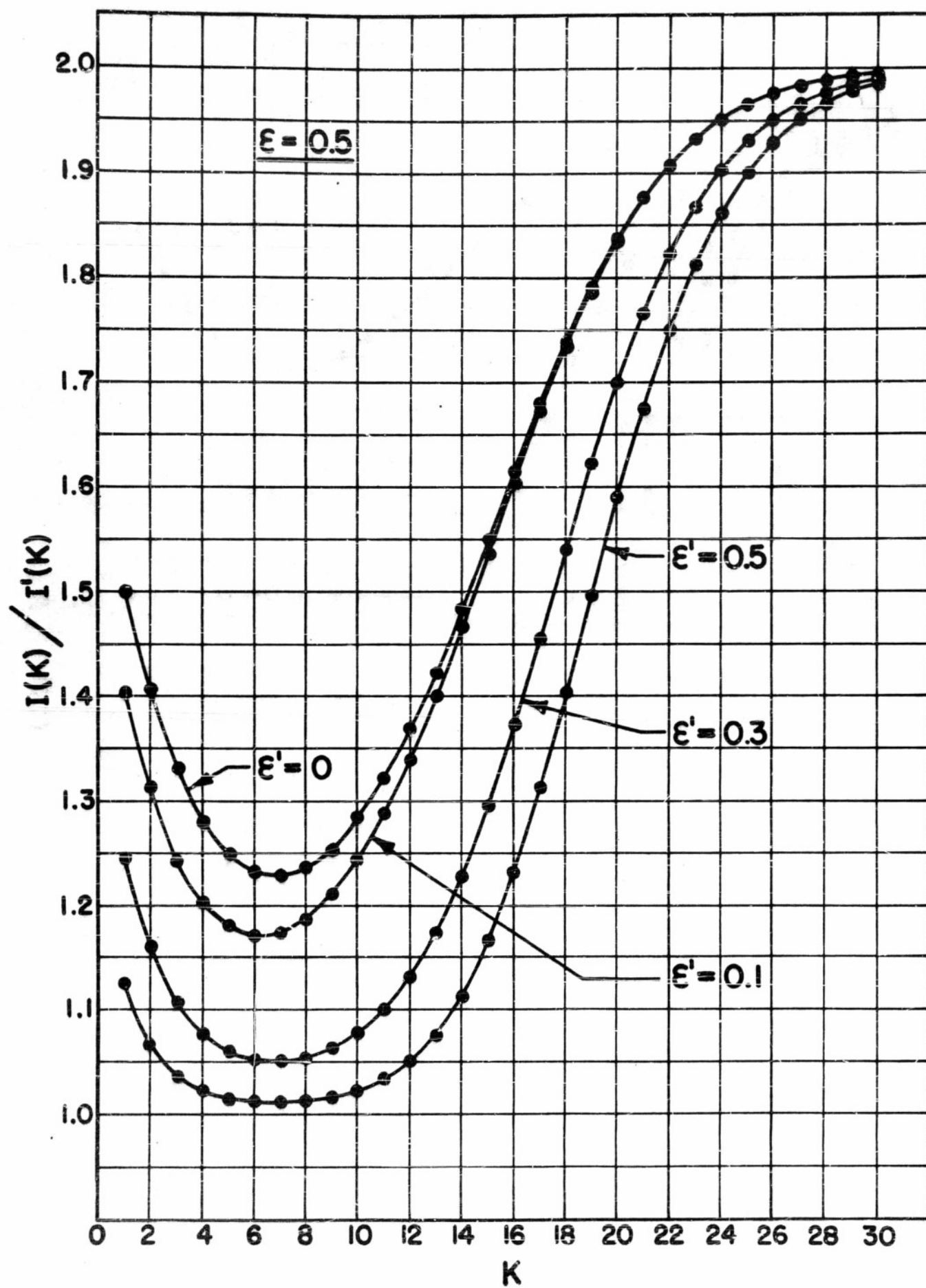
- Figure 1. The quantity $A(a, K)/A(a, K')$ as a function of K for $K' = 1$, $a = 0.005$.
- Figure 2. The quantity $A(a, K)/A(a, K')$ as a function of K for $K' = 1$, $a = 0.05$.
- Figure 3. The quantity $A(a, K)/A(a, K')$ as a function of K for $K' = 1$, $a = 2$.
- Figure 4. Schematic arrangement of two-path experiment for a flame represented by two isothermal regions.
- Figure 5. The quantity I/I' as a function of K for $\xi = 0.3$, $\xi' = 0$, 0.05, 0.10, and 0.3.
- Figure 6. The quantity I/I' as a function of K for $\xi = 0.5$, $\xi' = 0$, 0.10, 0.3, and 0.5.
- Figure 7. The quantity I/I' as a function of K for $\xi = 0.7$, $\xi' = 0$, 0.1, 0.3, 0.5, and 0.7.
- Figure 8. The quantity I/I' as a function of K for $\xi = 0.9$, $\xi' = 0$, 0.1, 0.3, 0.5, 0.7, and 0.9.
- Figure 9. Schematic arrangement of absorption experiment for a flame represented by two isothermal regions.
- Figure 10. The quantity $I(K)/I'(K)$ as a function of K for $\xi = 0.7$, $\xi' = 0.1$, $a = 0, 0.05, 0.3, 0.6, 2$, and 10.
- Figure 11. The quantity $I(K)/I'(K)$ as a function of K for $\xi = 0.7$, $\xi' = 0.1$, $a = 0, 0.05, 0.3, 0.6, 2$, and 10.

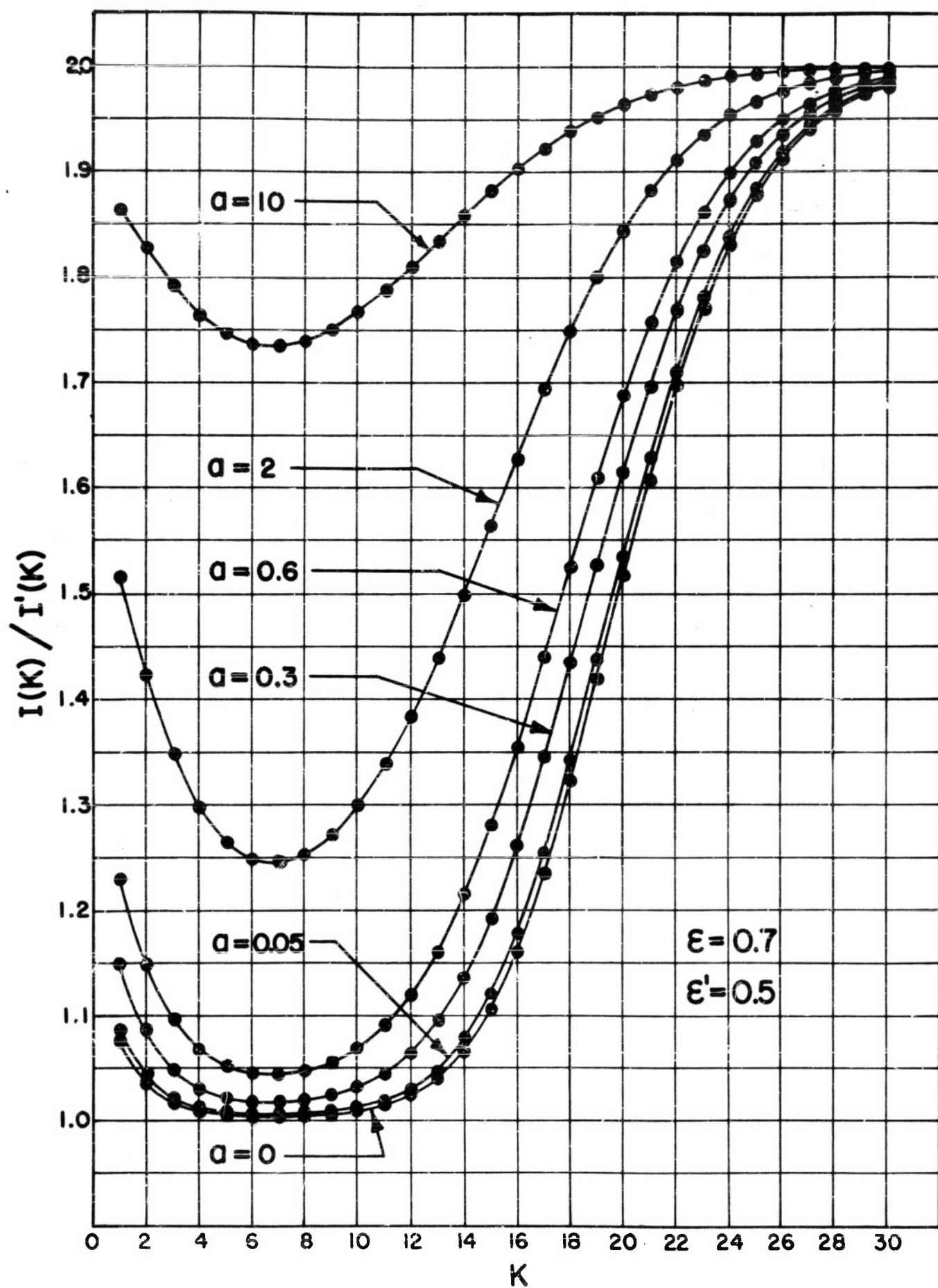


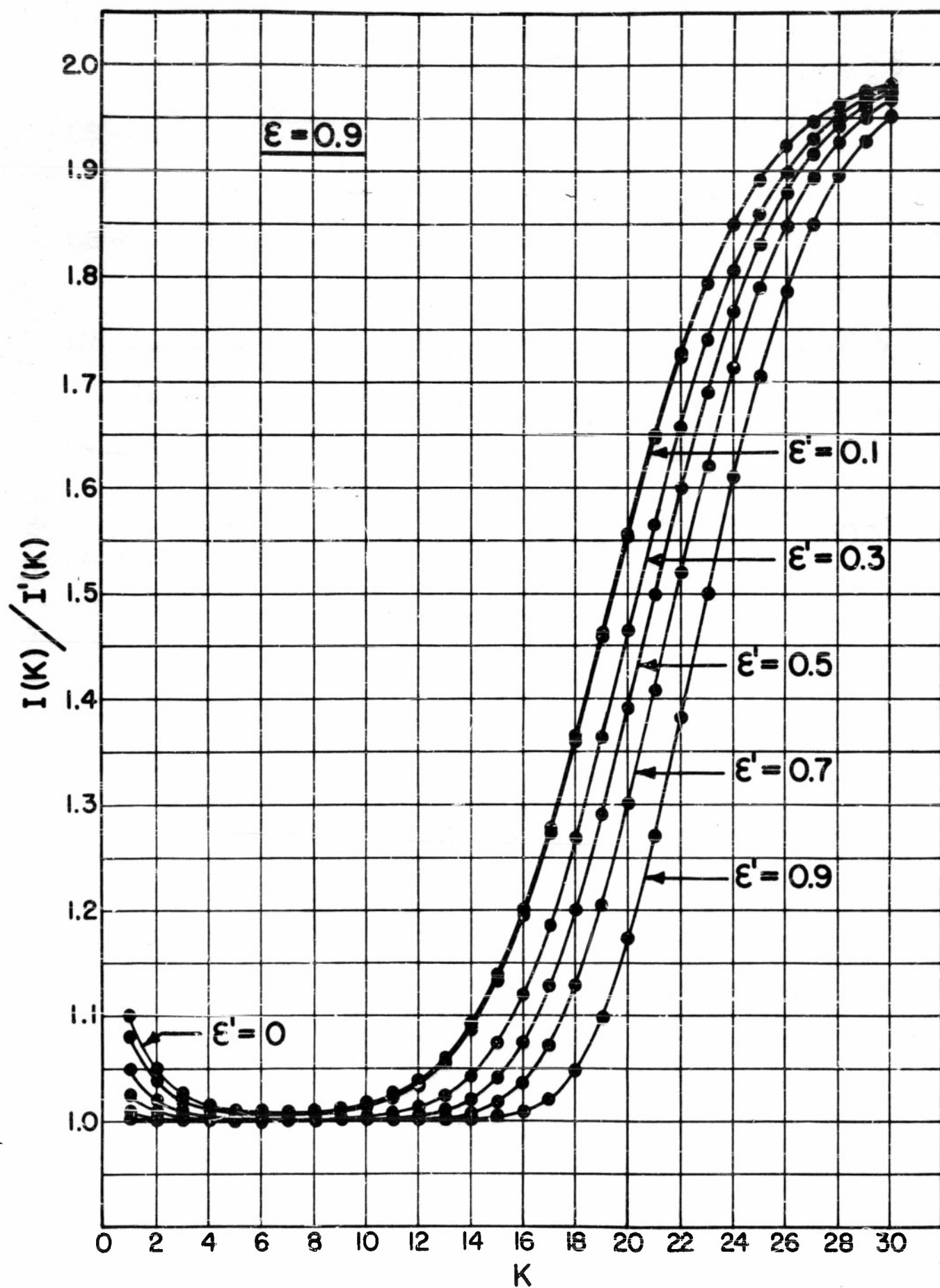


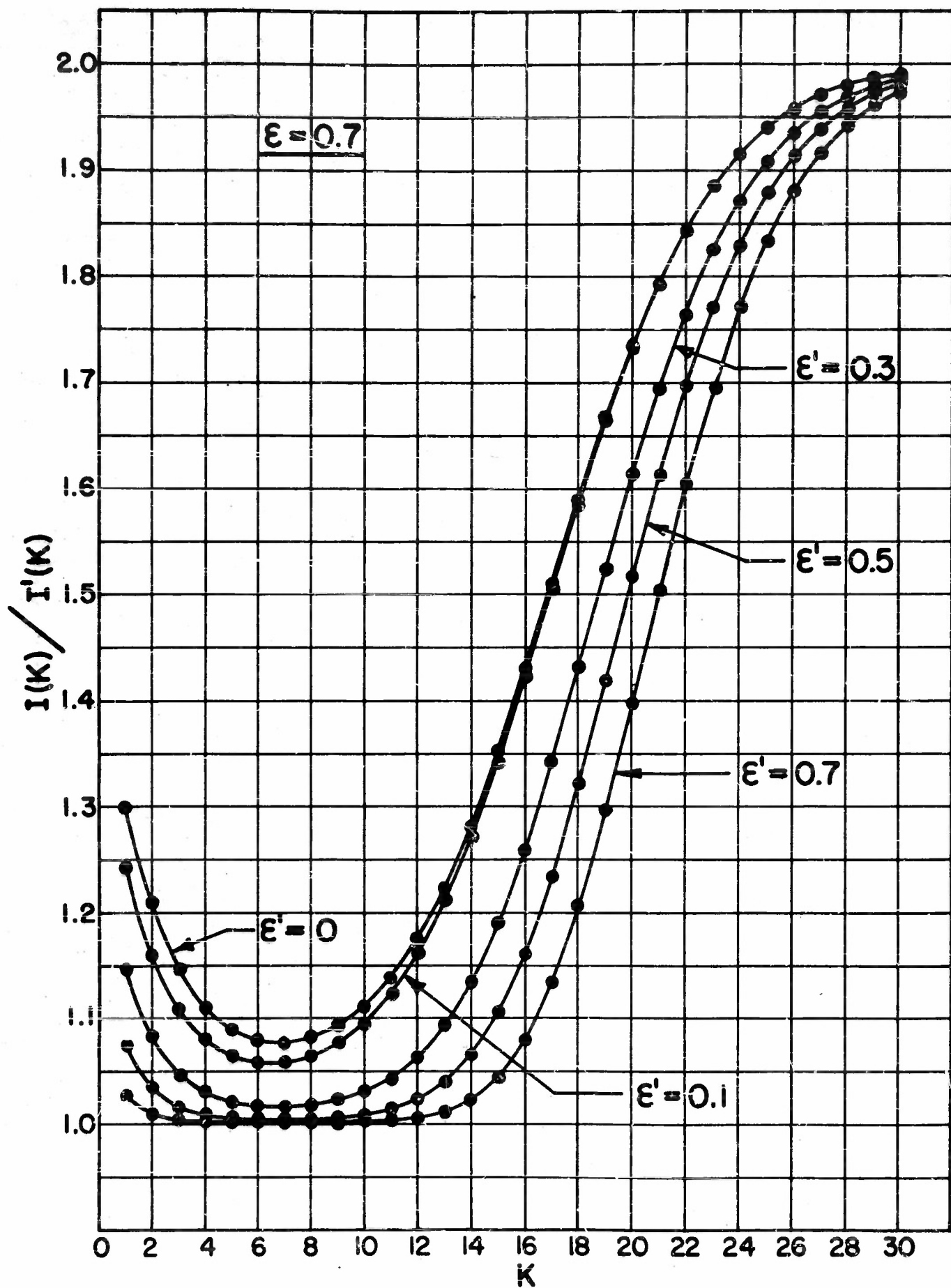


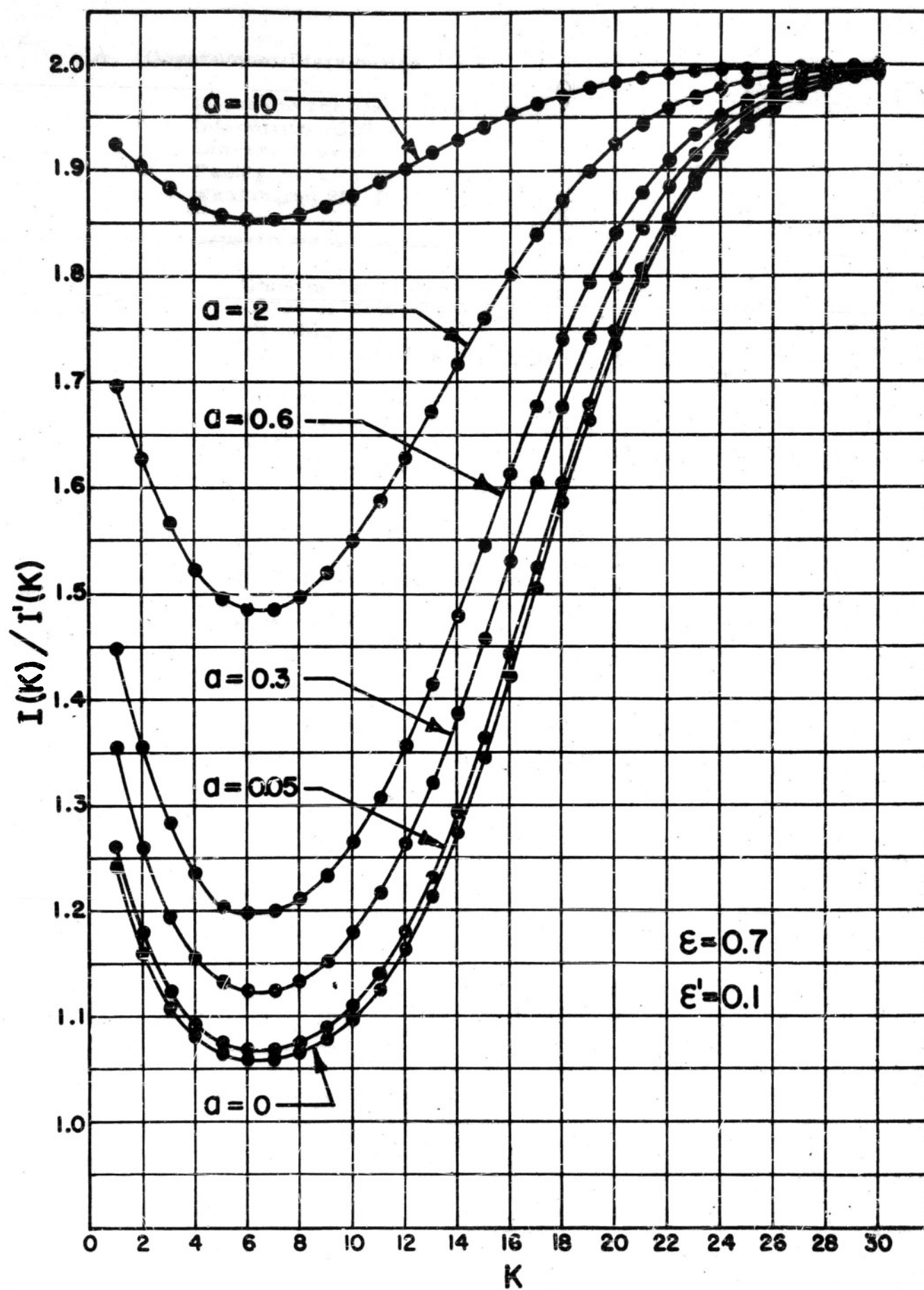












A. Government Distribution

**Research and Development Board
Information Office
Library Branch
Pentagon Building
Washington 25, D. C. (2 copies)**

Department of the Navy

**Chief of Naval Research
Office of Naval Research
Washington 25, D. C.
Attn: Physics Branch (Code 421) (2 copies)**

**Director, Naval Research Laboratory
Washington 25, D. C.
Attn: Technical Information Officer (Code 2000) (9 copies)
Attn: Code 2021 (2 copies)**

**Director
Office of Naval Research Branch Office
150 Causeway
Boston 10, Massachusetts (1 copy)**

**Director
Office of Naval Research Branch Office
346 Broadway
New York 13, New York (1 copy)**

**Director
Office of Naval Research Branch Office
American Fore Building
844 North Rush Street
Chicago 11, Illinois (1 copy)**

**Director
Office of Naval Research Branch Office
1000 Geary Street
San Francisco 9, California (1 copy)**

**Director
Office of Naval Research Branch Office
1031 East Green Street
Pasadena 1, California (1 copy)**

**Officer-in-Charge
Office of Naval Research
Navy No. 100, Fleet Post Office
New York, N. Y. (2 copies)**

Chief, Bureau of Aeronautics
Navy Department
Washington 25, D. C.
Attn: TD-4 (1 copy)

Chief, Bureau of Ordnance
Department of the Navy
Washington 25, D. C.
Attn: Technical Library, AD 3 (1 copy)

Chief, Bureau of Ships
Department of the Navy
Washington 25, D. C.
Attn: Code 324 (1 copy)

Director
Naval Research Laboratory
Washington 20, D. C.
Attn: Dr. J. A. Sanderson, Via Code 2021 (1 copy)
Dr. P. Egli " " " (1 copy)

Chief of Bureau of Ships
Navy Department
Washington 25, D. C.
Attn: Code 853 (1 copy)

Chief of Bureau of Aeronautics
Navy Department
Washington 25, D. C.
Attn: Code EL 421 (1 copy)
Code EL 454 (1 copy)

Commanding Officer
Naval Ordnance Test Station
Inyokern, California (1 copy)

Office of the Deputy Chief of Naval Operations
Logistics Section
Pentagon Building, Room 4A530
Washington 25, D. C.
Attn: LCDR W. A. Arthur (1 copy)

Director, Naval Ordnance Laboratory
White Oaks, Maryland
Attn: Physical Optics Division (1 copy)

Commander
Naval Air Missile Test Center
Director of Tests
Point Mugu
Port Hueneme, California (1 copy)

Commander
Naval Air Development Center (AEEL)
Johnsville, Pennsylvania (1 copy)

Department of Defense

**Research and Development Board
Committee on Electronics
Panel on Infrared
Pentagon Building
Washington 25, D. C. (2 copies)**

Department of Commerce

**Director
National Bureau of Standards
Washington 25, D. C. (2 copies)**

Department of the Air Force

**Commanding General
Air Material Command
Wright Patterson Air Force Base
Dayton, Ohio
Attn: Aircraft Radiation Lab. WCERD-3 (1 copy)
Armament Lab. WCLGB-2 (1 copy)**

Department of the Army

**Commanding General
Engineer Research and Development Laboratories
Fort Belvoir, Virginia
Attn: Technical Intelligence Branch (2 copies)**

**Evans Signal Laboratory
Physical Optics Section
Belmar, New Jersey
Attn: Mr. Harry Dauber (1 copy)**

**Office of Chief Signal Officer
Engineering and Technical Service
Pentagon Building, Room No. 3C-289
Washington, D. C.
Attn: SiGGG-S, Mr. N. Stulman (1 copy)**

**Office, Chief of Ordnance
Pentagon Building, Room 2D337
Washington 25, D. C.
Attn: Mr. J. E. Darr, ORDER (1 copy)**

**Office of Chief Army Field Forces
Development Section
Fort Monroe, Virginia
Attn: Lt. Col. A. J. Weinling (1 copy)**

**Office of Chief of Engineers
Department of the Army
Washington 25, D. C.
Attn: Mr. Henry T. Gibbs (1 copy)**

Non-Government Distribution

R. C. A. Laboratories
Princeton, New Jersey
Attn: Dr. G. A. Morton (1 copy)

Argonne National Laboratory
P. O. Box 5207
Chicago 80, Illinois
Attn: Dr. Hoylande D. Young (1 copy)

U. S. Atomic Energy Commission
1901 Constitution Avenue, N. W.
Washington 25, D. C.
Attn: B. M. Fry (1 copy)

Brookhaven National Laboratory
Technical Information Division
Upton, Long Island, New York
Attn: Research Library (1 copy)

Carbide and Carbon Chemicals Division
Central Reports and Information Office (Y-12)
P. O. Box P
Oak Ridge, Tennessee (1 copy)

Knolls Atomic Power Laboratory
P. O. Box 1072
Schenectady, New York
Attn: Document Librarian (1 copy)

Los Alamos Scientific Laboratory
P. O. Box 1663
Los Alamos, New Mexico
Attn: Document Custodian (1 copy)

Mound Laboratory
U. S. Atomic Energy Commission
P. O. Box 32
Miamisburg, Ohio

U. S. Atomic Energy Commission
New York Operations Office
P. O. Box 30, Ardenia Station
New York 23, New York
Attn: Division of Technical Information
and Declassification Service (1 copy)

Oak Ridge National Laboratory
P. O. Box P
Oak Ridge, Tennessee
Attn: Central Files (1 copy)

U. S. Atomic Energy Commission
Library Branch, Technical Information Division, ORE
P. O. Box E.
Oak Ridge, Tennessee (1 copy)

University of California Radiation Laboratory
Room 128, Building 50
Berkeley, California
Attn: Dr. R. K. Wakerling (1 copy)

Westinghouse Electric Corporation
Atomic Power Division
P. O. Box 1468
Pittsburgh 30, Pennsylvania
Attn: Librarian (1 copy)

Johns Hopkins University
Department of Physics
Baltimore, Maryland
Attn: Dr. G. H. Dieke (1 copy)
Attn: Dr. W. S. Benedict (1 copy)

Brandeis University
Waltham, Mass.
Attn: Dr. S. Golden (1 copy)

University of Minnesota
Department of Chemistry
Minneapolis, Minnesota
Attn: Dr. Bryce L. Crawford, Jr. (1 copy)

University of Chicago
Ryerson Physical Laboratory
Chicago, Illinois
Attn: Dr. R. S. Mulliken (1 copy)

Pennsylvania State College
Department of Physics
State College, Pennsylvania
Attn: Dr. D. H. Rank (1 copy)

Massachusetts Institute of Technology
Cambridge, Massachusetts
Department of Physics
Attn: Dr. John C. Slater (1 copy)
Department of Chemical Engineering
Attn: Dr. H. C. Hottel (1 copy)

University of California
Department of Physics
Berkeley 4, California
Attn: Dr. L. B. Loeb (1 copy)

University of Maine
Department of Physics
Orono, Maine
Attn: Dr. C. E. Bennett (1 copy)

Johns Hopkins University
Applied Physics Laboratory
8621 Georgia Ave.
Silver Spring, Maryland
Attn: Dr. S. Silverman (1 copy)

Office of Naval Research
1030 East Green St
Pasadena 1, California
Attn: Dr. Warren Arnquist (1 copy)

University of Michigan
Department of Physics
Ann Arbor, Michigan
Attn: Dr. G. B. B. M. Sutherland (1 copy)

Ohio State University
Department of Physics
Columbus, Ohio
Attn: Dr. H. H. Nielsen (1 copy)

Cornell University
Ithaca, New York
Attn: Dr. S. H. Bauer (1 copy)

University of Utah
Department of Physics
Salt Lake City, Utah
Attn: Dr. W. M. Elsasser (1 copy)

Princeton University
Princeton, New Jersey
Attn: Dr. M. Summerfield (1 copy)

Imperial College
London, England
Department of Chemical Engineering
Attn: Dr. A. G. Gaydon (1 copy)

National Research Council
Ottawa, Ontario, Canada
Attn: Dr. G. Herzberg (1 copy)

University of Wisconsin
Department of Chemistry
Madison, Wisconsin
Attn: Dr. J. O. Hirschfelder (1 copy)

University of Michigan Observatory
Ann Arbor, Michigan
Attn: Dr. L. Goldberg (1 copy)

Dr. A. O. Dekker
Aerojet Engineering Corporation
Azusa, California (1 copy)

California Institute of Technology
Pasadena, California
Engineering Division
Attn: Dr. F. C. Lindvall (1 copy)
Astrophysics Department
Attn: Dr. J. L. Greenstein (1 copy)
Department of Chemistry
Attn: Dr. R. M. Badger (1 copy)
Attn: Dr. O. R. Wulf (1 copy)
Jet Propulsion Laboratory
Attn: Dr. L. G. Dunn (1 copy)
~~Guggenheim Jet Propulsion Center~~
Attn: Dr. H. S. Tsien (1 copy)
Attn: Dr. S. S. Penner (1 copy)